國 立 交 通 大 學

電機學院 電信學程

碩 士 論 文

用於主動消噪系統之新可變長度與步階大小的 FXLMS 演算法

Active Noise Cancellation with a New Variable Tap Length and Step Size FXLMS Algorithm

研 究 生：楚 斐 韜

指導教授：吳 文 榕 博士

張 大 中 博士
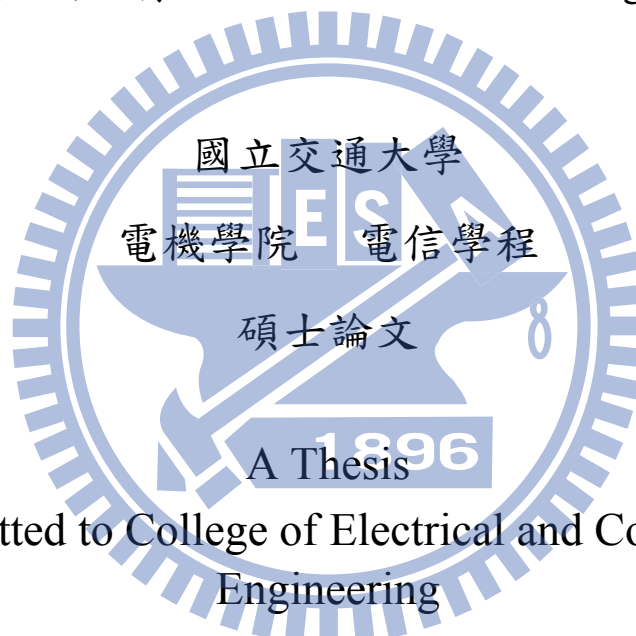
中 華 民 國 一 百 零 二 年 一 月

用於主動消噪系統之新可變長度與步階大小的 FXLMS 演算法

Active Noise Cancellation with a New Variable Tap Length and Step Size FXLMS Algorithm

研 究 生： 楚斐韜　　　　　Student: Fei-Tao Chu

指導教授： 吳文榕　博士　　Advisor: Wen-Rong Wu, Ph.D.
　　　　　張大中　博士　　　　　　　Dah-Chung Chang, Ph.D.

國 立 交 通 大 學

電 機 學 院　　電 信 學 程

碩 士 論 文

A Thesis

Submitted to College of Electrical and Computer Engineering

National Chiao Tung University

in Partial Fulfillment of the Requirements

for the Degree of

Master of Science

in

Communication Engineering

Jan 2013

Hsinchu, Taiwan, Republic of China

中 華 民 國 一 百 零 二 年 一 月

用於主動消噪系統之新可變長度與步階大小的 FXLMS 演算法

研究生：楚斐韜　　　　　　　　指導教授：吳文榕　博士
　　　　　　　　　　　　　　　　　　　　張大中　博士

國立交通大學　　電機學院　　電信學程　　碩士班

摘　要

　　FxLMS 演算法已廣泛的使用於主動消噪系統 (ANC)，之前一些不同版本的 FxLMS 演算法已研究過如何減少計算複雜度或增進收斂速度。在一般的應用上，傳統的 FxLMS 演算法雖其結構可能容易實現，但因使用的濾波器長度較長，故其收斂速度十分緩慢。在本篇論文中，提出新的可變長度及步階大小之 FxLMS 演算法用於消噪系統。有鑑於低通濾波器在消噪系統第二路徑的影響，控制濾波器的脈衝響應之包跡以非對稱指數衰減函數來模擬，用以發展我們的演算法。模擬結果顯示，相較於固定長度的 FxLMS 演算法與先前提出的可變步階大小的 FxLMS 演算法，此一演算法確實能夠顯著的改進收斂速度及訊噪比。

Active Noise Cancellation with a New Variable Tap Length and Step Size FXLMS Algorithm

Student:Fei-Tao Chu   Adivisor:Wen-Rong Wu, Ph.D.

Dah-Chung Chang, Ph.D.

Degree Program of Electrical and Computer Engineering

National Chiao Tung University

ABSTRACT

The filtered-X least mean square (FxLMS) algorithm is widely used for active noise cancellation (ANC). Some variants of FxLMS algorithms have been studied to reduce computational complexity or to improve convergence rate. In general applications, a long tap length is usually required for the conventional FxLMS method which convergence rate is very slow though its structure is possibly very easy to implement. In this paper, a new ANC system is proposed with a variable tap length and step size FxLMS algorithm. Taking into account the effect of the lowpass filter in the secondary path of an ANC system, the impulse response of the control filter is modeled with an unsymmetric and exponential decay-

ing envelope to develop our algorithm. Simulation results show that the

proposed algorithm does provide a significant performance improvement

on convergence rate and noise reduction ratio compared to the fixed tap

FxLMS and previously proposed variable step size FxLMS algorithms.

Acknowledgement

It is really a long journey to complete my thesis. First of all, I sincerely express my gratitude to my thesis advisors, Prof. Wen-Rong Wu and Prof. Dah-Chung Chang, for their guidance and direction. In addition, the reviewer, Prof. Ta-Sung Lee, offered his precious advice on my thesis, which inspired me very much. In this year, my family's and friends' support and encouragement are highly appreciated.
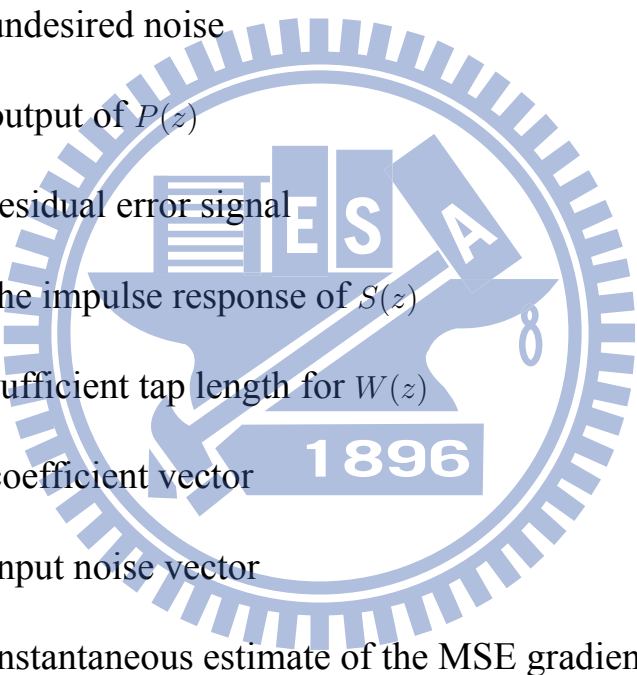
Contents

List of Figures

Symbol Description

$P(z)$:   unknown plant

$S(z)$:   secondary path

$W(z)$:   adaptive filter

$v(n)$:   unwanted background noise

$x(n)$:   undesired noise

$d(n)$:   output of $P(z)$

$e(n)$:   residual error signal

$s(n)$:   the impulse response of $S(z)$

K :   sufficient tap length for $W(z)$

$\mathbf{w}(n)$:   coefficient vector

$\mathbf{x}(n)$:   input noise vector

$\widehat{\xi}(n)$:   instantaneous estimate of the MSE gradient at time n

$\widehat{S}(z)$:   estimated of secondary path

$\widehat{s}(n)$:   estimated impulse response of $\widehat{S}(z)$

$x'(n)$:   the output of $\widehat{S}(z)$

P_x :   the power of the input signal $x(n)$

Δ :   accounts for the secondary path delay

$W^o(z)$:   optimal of adaptive filter $W(z)$

M	:	the left tap length of the maximum output impulse response
N	:	right tap length including the maximum output impulse response
$\mathbf{w}_K^o$	:	the optimal coefficients for $W(z)$
τ_1	:	left decaying factor
τ_2	:	right decaying factor
$r_w(i)$	:	zero-mean i.i.d. Gaussian random sequence
$\sigma_{r_w}^2$	:	variance of zero-mean i.i.d. Gaussian random sequence
$L(n)$	:	left hand-sides tap length at time n
$R(n)$	:	right hand-side tap length at time n
$\mu(n)$	:	step size at time n
$\mathbf{g}_K(n)$	:	total coefficients error
$\Lambda(n)$	:	the MSD of $\mathbf{g}_K(n)$
$\|.\|_2^2$	:	ℓ_2 norm
$E[\cdot]$	:	taking expectation
σ_x^2	:	variances of $x(n)$
σ_v^2	:	variances of $v(n)$
$\sigma_{x'}^2$	:	variances of $x'(n)$
σ_e^2	:	variances of $e(n)$
$\varepsilon(n)$	:	auxiliary noise
$u(n)$	:	the output of $S(z)$ by $\varepsilon(n)$

$\hat{u}(n)$: the output of $\widehat{S}(z)$ by $\varepsilon(n)$

$\xi(n)$: convolution output of the auxiliary noise $\varepsilon(n)$ and the

deviation of $\widehat{S}(z)$

σ_ξ^2 : variances of $\xi(n)$

$\rho(n)$: weighting factor

Chapter 1   Introduction

1.1   Review and Background

The acoustic noise reduction problem [1] [2] has been explored for many years, which is widely used in headphones, mobile phones, automobiles, and some industries which need to remedy the circumstance of noise disturbance. Instead of using passive methods, the active noise cancellation (ANC) system improves the efficiency in noise control with lower volume and cost. One of most widely used algorithms for the broadband ANC system is the filtered-X LMS (FxLMS) algorithm [3]. The FxLMS algorithm uses secondary path modeling and a control filter to compensate for uncertain effects in the system, e.g., ADC, DAC, error microphone, pre-amplifier, etc., because the FxLMS algorithm can lead to smaller residual noise in the broadband ANC system.

The FxLMS algorithm used for ANC has some variants such as the lattice ANC [4], frequency domain ANC, delayless subband ANC [5] [6], etc. The lattice structure filter fails to provide a satisfying convergence rate when the primary noise is broadband. Although the LMS processing in frequency domain or subband turns to obtain a faster convergence rate than the conventional time domain processing, it requires an additional

complexity to implement the discrete-time Fourier transform (DFT) or filter banks. Compared with the above variants, the transversal filter structure is relatively simple but a long tap length is required such that the maximum step size is limited in the FxLMS algorithm and consequently, the convergence rate is significantly slow [7] [8]. To remain the advantage of the simple LMS algorithm while increase the convergence rate, we develop a new variable tap length and step size FxLMS algorithm for ANC. In the literature, there are some existing variable tap length LMS algorithm [9] [10] [11], which considered a constant exponential decay envelope for the unknown impulse response plant in a system identification model. Based on minimizing the mean square deviation (MSD) of filter coefficients, the principle of the variable tap length algorithm is to first approach the modeled part of the plant's impulse response with a smaller tap length for using a larger step size which value is inverse to the tap length. Then, the tap length is progressively increased and finally converged to satisfy the minimum MSD criterion with a continuously decreasing step size. Hence, a fast convergence rate can be obtained.

For the application of ANC, the secondary path contains a lowpass filter model that results in a double-sided decaying envelope for the impulse response. However, the maximum output of the unknown primary plant is not necessarily at the middle of the impulse response. Hence, in or-

der to develop a new variable tap length FxLMS algorithm for ANC, we consider the unsymmetric and double-sided exponential decay impulse response in our case. The adaptation method for the variable step size is also developed in this thesis. Moreover, we propose a recursive form for optimal tap length estimation in order to simplify the computational complexity. Numerical results show that the new variable tap length and step size FxLMS algorithm has a fast convergence rate compared to the conventional FxLMS and variable step size algorithms. From the evaluation of noise reduction for ANC, the proposed algorithm achieves a better convergence performance than other compared methods as well.

1.2   Organization

The rest of this thesis is organized as follows: Chapter 2 describes the basic ANC system model. The proposed variable tap length and step size algorithm is addressed in Chapter 3, where a recursive form for variable tap length estimation and the convergence problem are also mentioned. In Chapter 4, we discuss how to achieve in the real system and the application for online secondary path estimation. The simulation results are collected in Chapter 5 and the conclusion is drawn in Chapter 6.

Chapter 2 The FxLMS ANC System

A general ANC system using the FxLMS algorithm is depicted in Fig. 2.1, in which $P(z)$ is an unknown plant in the primary path modeling the acoustic response from the reference microphone to the error microphone and an adaptive filter $W(z)$ in the secondary path is used to compensate for the loudspeaker system $S(z)$ to cancel an undesired noise $x(n)$ through $P(z)$. The unwanted background noise $v(n)$ is usually uncorrelated to $x(n)$ and added to the cancellation error signal. In this model, the objective of $W(z)$ is to minimize the residual error signal $e(n)$. Denote by $d(n)$ the output of $P(z)$ and $s(n)$ the impulse response of $S(z)$. Consider that K is a sufficient tap length for $W(z)$, the coefficient vector of $W(z)$ at time index n is $\mathbf{w}(n) = [w_0(n)\ w_1(n)\ \cdots\ w_{K-1}(n)]^T$, and the input noise vector $\mathbf{x}(n) = [x(n)\ x(n-1)\ \cdots\ x(n-K+1)]^T$. The residual error signal can be expressed as

$$e(n) = d(n) - [\mathbf{x}^T(n)\mathbf{w}(n)] * s(n) + v(n), \tag{2.1}$$

where $*$ denotes linear convolution.

The LMS algorithm can be used to find the recursive solution to $\mathbf{w}(n)$ based on minimizing the mean square error (MSE). Let $\xi(n) = e^2(n)$, the adaptive filter $\mathbf{w}(n)$ is then updated in the negative gradient direction with
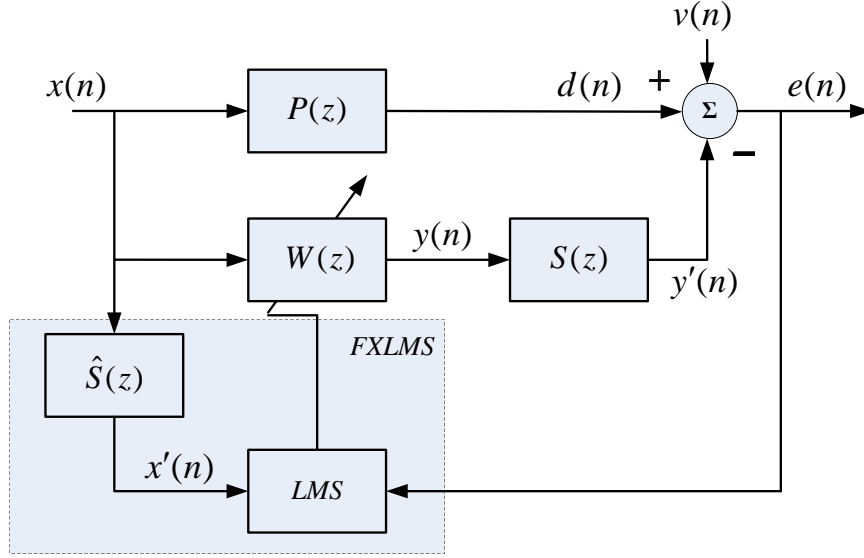
Figure 2.1: Block diagram of ANC system using the FXLMS algorithm.

step size μ as

$$\mathbf{w}(n+1) = \mathbf{w}(n) - \frac{\mu}{2}\nabla\widehat{\xi}(n) \qquad (2.2)$$

where $\widehat{\xi}(n)$ is an instantaneous estimate of the MSE gradient at time n with $\nabla\widehat{\xi}(n) = 2[\nabla e(n)]e(n)$. From (2.1), we have

$$\nabla e(n) = -s(n) * \mathbf{x}(n) = -\mathbf{x}'(n) \qquad (2.3)$$

where $\mathbf{x}'(n) = [x'(n)\ x'(n-1)\ \cdots\ x'(n-K+1)]^T$. Therefore, we have

$$\nabla\widehat{\xi}(n) = -2\mathbf{x}'(n)e(n). \qquad (2.4)$$

5

Substituting (2.4) into (2.2), we have the updated equation of $\mathbf{w}(n)$,

$$\mathbf{w}(n+1) = \mathbf{w}(n) + \mu\mathbf{x}'(n)e(n). \tag{2.5}$$

From (2.5), the transfer function $S(z)$ of the secondary path exists in the updated equation of adaptive filter coefficients and is conventionally called FxLMS algorithm. It is worth to note that $S(z)$ is usually unknown, so it should be modeled by filter $\widehat{S}(z)$, as shown in Fig.2.1. That is,

$$x'(n) = \widehat{s}(n) * x(n), \tag{2.6}$$

where $\widehat{s}(n)$ is the estimated impulse response of $\widehat{S}(z)$. Without loss of generality, we simply treat $\widehat{S}(z) = S(z)$ in this work. The online secondary path modeling and estimation methods can be referred to [8] [12].

In a typical ANC system, the length of the impulse responses of unknown plant and secondary path may be very long, which directly affects the tap length of the adaptive filter. As mentioned in [2], the range of the step size is

$$0 < \mu < \frac{2}{P_x(K + 2 + 2\Delta)}, \tag{2.7}$$

where P_x is the power of the input signal $x(n)$ for $P(z)$ and Δ accounts for the secondary path delay. When the tap length is long, the convergence

speed becomes small because of a very small step size. Consequently, a variable length and step size LMS algorithm is studied in order to improve the ANC system.

Chapter 3   The New Variable Tap Length and Step Size FxLMS Algorithm for ANC

3.1   Proposed Algorithm

From (2.1), the z-transform of the residual error signal is

$$E(z) = [P(z) - W(z)S(z)]X(z) + V(z). \tag{3.1}$$

As ignoring $V(z)$, a simple insight into (3.1) is that the residual error is close to zero, i.e., $E(z) = 0$, after the adaptive filter converges. Hence, we can see that the control filter $W(z)$ is to realize the optimal transfer function with

$$W^o(z) = \frac{P(z)}{S(z)}. \tag{3.2}$$

In some circumstances, the power profiles of the impulse responses of $P(z)$ and $S(z)$ may have exponentially decaying envelopes on both sides of the maximum output response. For example, the loudspeaker system model $S(z)$ includes the D/A converter, reconstruction filter, power amplifier, etc., in which the lowpass reconstruction filter usually consists of symmetric filter coefficients for a linear-phase concern. However, the

$P(z)$ may have an unsymmetric decaying envelope. Here, we assume that the impulse response of $W(z)$ also has an unsymmetric decaying envelope, where the left tap length of the maximum output impulse response is M while the right one is N including the maximum output impulse response. We express the optimal coefficients for $W(z)$ as follows:

$$\mathbf{w}_K^o = [w_{-M}^o \quad \cdots \quad w_{-1}^o \quad w_0^o \quad w_1^o \cdots w_{N-1}^o]^T \tag{3.3}$$

and the following exponential function is used to model the envelope of the impulse response coefficients

$$w_i^o = \begin{cases} e^{i\tau_1} r_w(i), & i = -M, \cdots, -1 \\ e^{-i\tau_2} r_w(i), & i = 0, 1, \cdots, N-1, \end{cases} \tag{3.4}$$

where $i = -M, \cdots, -1, 0, 1, \cdots, N-1$, the decaying factor τ_1 and τ_2 are positive constants, and $r_w(i)$ is a zero-mean i.i.d. Gaussian random sequence with variance $\sigma_{r_w}^2$.

The proposed FxLMS algorithm adaptively adjusts its tap length and step size as time progresses. Denote by $L(n)$, $R(n)$ and $\mu(n)$ the left hand-sides tap length, right hand-side tap length and step size at time n, respectively, and $L(n) + R(n) \leq K$. Using the notation $L(n) + R(n)$ for the subscript of $\mathbf{w}_{L(n)+R(n)}(n)$ and $\mathbf{x}'_{L(n)+R(n)}(n)$ to represent $L(n) + R(n)$-tap fil-

ter vector and input vector, respectively, and $\mathbf{w}_{L(n)+R(n)}(n) = [w_{-L(n)}(n) \cdots$
$w_{-1}(n) \, w_0(n) \, w_1(n) \cdots w_{R(n)-1}(n)]^T$ and $\mathbf{x}'_{L(n)+R(n)}(n) = [x'(n + L(n)) \cdots x'(n + 1) \, x'(n) \, x'(n-1) \cdots x'(n - R(n) + 1)]^T$, we can rewrite (2.5) as

$$\begin{bmatrix} \mathbf{w}_{L(n+1)}(n+1) \\ \\ \mathbf{w}_{R(n+1)}(n+1) \end{bmatrix} = \begin{bmatrix} \mathbf{0}_{L(n+1)-L(n)} \\ \mathbf{w}_{L(n)}(n) \\ \mathbf{w}_{R(n)}(n) \\ \mathbf{0}_{R(n+1)-R(n)} \end{bmatrix} + \mu(n+1)e(n)\mathbf{x}'_{L(n+1)+R(n+1)}(n). \; (3.5)$$

Here, we assume that the modeled part of $W(z)$ is expanded from the maximum impulse response of the filter, that is, $\mathbf{w}_K(n) = [\mathbf{0}_L^T \; \mathbf{w}_{L(n)+R(n)}^T(n) \; \mathbf{0}_R^T]^T$ where the left $\mathbf{0}_L$ denotes the $1 \times (M - L(n))$ zero vector and the right $\mathbf{0}_R$ denotes the $1 \times (N - R(n))$ zero vector. Now, split $\mathbf{w}_{M+N}^o$ into four parts as

$$\mathbf{w}_K^o = \begin{bmatrix} {\mathbf{w}_{M-L(n)}^o}' \\ \mathbf{w}_{L(n)}^o \\ \mathbf{w}_{R(n)}^o \\ {\mathbf{w}_{N-R(n)}^o}'' \end{bmatrix}, \tag{3.6}$$

10

and define the total coefficients error as

$$\mathbf{g}_K(n) = \begin{bmatrix} \mathbf{0}_{M-L(n)} \\ \mathbf{W}_{L(n)}(n) \\ \mathbf{W}_{R(n)}(n) \\ \mathbf{0}_{N-R(n)} \end{bmatrix} - \mathbf{w}_K^o. \tag{3.7}$$

From (3.2), we can express the output of $P(z)$ as

$$d(n) = [\mathbf{x}_K^T(n) \ \mathbf{w}_K^o] * s(n). \tag{3.8}$$

Substituting (3.8) into (2.1) and using (3.7), the residual error signal becomes

$$
\begin{aligned}
e(n) &= [\mathbf{x}_K^T(n)\mathbf{w}_K^o - \mathbf{x}_{L(n)+R(n)}^T(n)\mathbf{w}_{L(n)+R(n)}(n)] \\
&\quad *s(n) + v(n) \\
&= -[\mathbf{x}_K^T(n)\mathbf{g}_K(n)] * s(n) + v(n) \\
&= -\mathbf{x}'^T_K(n)\mathbf{g}_K(n) + v(n).
\end{aligned}
\tag{3.9}
$$

Substituting $e(n)$ in (3.5) with (3.9) and subtracting $\mathbf{w}_K^o$ at both sides of

11

(3.5), we obtain

$$\mathbf{g}_K(n+1) = \mathbf{A}(n)\mathbf{g}_K(n) + \mu(n+1)v(n) \begin{bmatrix} \mathbf{0}_{M-L(n+1)} \\ \mathbf{x'}_{L(n+1)}(n) \\ \mathbf{x'}_{R(n+1)}(n) \\ \mathbf{0}_{N-R(n+1)} \end{bmatrix}, \qquad (3.10)$$

where

$$\mathbf{A}(n) = \mathbf{I}_K - \mu(n+1) \begin{bmatrix} \mathbf{0}_{M-L(n+1)} \\ \mathbf{x'}_{L(n+1)}(n) \\ \mathbf{x'}_{R(n+1)}(n) \\ \mathbf{0}_{N-R(n+1)} \end{bmatrix} \mathbf{x'}_K^T(n), \qquad (3.11)$$

and $\mathbf{I}_K$ is the $K \times K$ identity matrix.

To develop the recursive algorithm for $L(n+1)$, $R(n+1)$ and $\mu(n+1)$, the MSD of $\mathbf{g}_K(n)$ is explored. Define

$$\Lambda(n) \equiv E[\|\mathbf{g}_K(n)\|_2^2], \qquad (3.12)$$

where $\|.\|_2^2$ denotes ℓ_2 norm and $E[\cdot]$ represents taking expectation. Assume that $x(n)$ and $v(n)$ are two i.i.d. Gaussian sequences with variances σ_x^2 and σ_v^2, respectively. According to the similar assumption and analysis [9],

12

we have

$$\Lambda(n + 1) = \eta(n + 1)\Lambda(n) + (\beta(n + 1) - \eta(n + 1))\Gamma(n + 1) + \gamma(n + 1), \quad (3.13)$$

where

$$\Gamma(n + 1) = E\left[\left\|\mathbf{w}^o_{M-L(n+1)}{}'\right\|^2_2\right] + E\left[\left\|\mathbf{w}^o_{N-R(n+1)}{}''\right\|^2_2\right]$$

$$(3.14)$$

$$\eta(n + 1) = 1 - 2\mu(n + 1)\sigma^2_{x'} + (L(n + 1) + R(n + 1) + 2)$$

$$\times \mu^2(n + 1)\sigma^4_{x'}, \quad (3.15)$$

$$\beta(n + 1) = 1 + (L(n + 1) + R(n + 1))\mu^2(n + 1)\sigma^4_{x'}, \quad (3.16)$$

$$\gamma(n + 1) = (L(n + 1) + R(n + 1))\mu^2(n + 1)\sigma^2_{x'}\sigma^2_v, \quad (3.17)$$

and using (3.4) for $\mathbf{w}^o_K$, we have

$$E[\|\mathbf{w}^o_{M-L(n+1)}{}'\|^2_2] = \frac{1 - e^{2(M-L(n+1))\tau_1}}{1 - e^{2M\tau_1}} E[\|\mathbf{w}^o_M\|^2_2], \quad (3.18)$$

$$E[\|\mathbf{w}^o_{N-R(n+1)}{}''\|^2_2] = \frac{e^{-2R(n+1)\tau_2} - e^{-2N\tau_w}}{1 - e^{-2N\tau_2}} E[\|\mathbf{w}^o_N\|^2_2], \quad (3.19)$$

where

$$E[\|\mathbf{w}_M^o\|_2^2] = \frac{e^{-2M\tau_1}\left(1 - e^{2M\tau_1}\right)}{1 - e^{2\tau_1}}\sigma_{r_w}^2, \qquad (3.20)$$

$$E[\|\mathbf{w}_N^o\|_2^2] = \frac{1 - e^{-2N\tau_2}}{1 - e^{-2\tau_2}}\sigma_{r_w}^2. \qquad (3.21)$$

Substituting (3.14), (3.18), (3.19), (3.20) and (3.21) into (3.13), the MSD can be rewritten as

$$\Lambda(n+1) = \eta(n+1)\Lambda(n) + (\beta(n+1) - \eta(n+1))$$
$$\times \left(\frac{e^{-2M\tau_1} - e^{-2L(n+1)\tau_1}}{1 - e^{2\tau_1}} + \frac{e^{-2R(n+1)\tau_2} - e^{-2N\tau_2}}{1 - e^{-2\tau_2}}\right)\sigma_{r_w}^2$$
$$+ \gamma(n+1). \qquad (3.22)$$

The optimal tap length and step size can be found by minimizing the MSD with respect to $L(n+1)$, $R(n+1)$ and $\mu(n+1)$. Therefore, taking the first-order derivative of $\Lambda(n+1)$ with respect to $L(n+1)$, $R(n+1)$ and $\mu(n+1)$, respectively, and setting $\frac{\partial\Lambda(n+1)}{\partial L(n+1)}$, $\frac{\partial\Lambda(n+1)}{\partial R(n+1)}$ and $\frac{\partial\Lambda(n+1)}{\partial\mu(n+1)}$ to zero, after some mathematical manipulation we obtain

$$L(n+1) = -\frac{1}{2\tau_1}\ln\frac{\mu(n+1)(\sigma_{x'}^2\Lambda(n) + \sigma_v^2)(1 - e^{2\tau_1})}{-4\tau_1(1 - \mu(n+1)\sigma_{x'}^2)\sigma_{r_w}^2}, \qquad (3.23)$$

$$R(n+1) = -\frac{1}{2\tau_2} \ln \frac{\mu(n+1)(\sigma_{x'}^2 \Lambda(n) + \sigma_v^2)(1 - e^{-2\tau_2})}{4\tau_2(1 - \mu(n+1)\sigma_{x'}^2)\sigma_{r_w}^2}, \tag{3.24}$$

and

$$\mu(n+1) = \frac{1 - \frac{\Gamma(n+1)}{\Lambda(n)}}{(L(n+1) + R(n+1) + 2)\sigma_{x'}^2 + \frac{(L(n+1)+R(n+1))\sigma_v^2 - 2\sigma_{x'}^2\Gamma(n+1)}{\Lambda(n)}}. \tag{3.25}$$

We have to mention that (3.23), (3.24) and (3.25) are required to be solved simultaneously for $L(n+1)$, $R(n+1)$ and $\mu(n+1)$. It is a tough work to get the closed-form solution of the joint equations. Taking into consideration a quasi-static assumption for $L(n) \approx L(n+1)$ and $R(n) \approx R(n+1)$ [11], a suboptimal solution can be efficiently found by replacing $L(n+1)$ and $R(n+1)$ by $L(n)$ and $R(n)$ in (3.25). That is,

$$\mu(n+1) = \frac{1 - \frac{\Gamma(n)}{\Lambda(n)}}{(L(n) + R(n) + 2)\sigma_{x'}^2 + \frac{(L(n)+R(n))\sigma_v^2 - 2\sigma_{x'}^2\Gamma(n)}{\Lambda(n)}}. \tag{3.26}$$

From (3.26) we can observe that when $v(n)$ is ignored and the adaptive filter approaches the perfect tap length, $\sigma_v^2 = \Gamma(n) = 0$ and thus $\mu(n+1) \approx \frac{1}{(K+2)\sigma_{x'}^2}$, which is consistent with the convergence condition (2.7) excluding the effect of $S(z)$ according to (3.2). Therefore, an alternating calculation by (3.23), (3.24) and (3.26) can be used for $L(n+1)$, $R(n+1)$ and $\mu(n+1)$.

3.2 Recursive Form and Convergence

The more useful results in using (3.23) and (3.24) are to develop their alternatives of recursive forms. First, as mentioned in [10], it can be shown that $\sigma_e^2(n) = \sigma_{x'}^2 \Lambda(n) + \sigma_v^2$. After re-manipulating (3.26), we have

$$
\begin{aligned}
\mu(n+1) &= \frac{\Lambda(n) - \Gamma(n)}{2\sigma_{x'}^2(\Lambda(n) - \Gamma(n)) + (L(n) + R(n))\sigma_e^2(n)} \\
&= \frac{1}{2\sigma_{x'}^2 + (L(n) + R(n))\Phi(n)}
\end{aligned}
\tag{3.27}
$$

where

$$
\Phi(n) = \frac{\sigma_e^2(n)}{\Lambda(n) - \Gamma(n)}.
\tag{3.28}
$$

Moreover, from (3.6), (3.7), and (3.12), we can prove that

$$
\Lambda(n) - \Gamma(n) = E[\|\mathbf{g}_{L(n)+R(n)}(n)\|_2^2].
\tag{3.29}
$$

Now, let us move on writing the result of $L(n+1) - L(n)$ and $R(n+1) - R(n)$ based on (3.23) and (3.24). Note that although $\sigma_e^2(n)$ varies and actually vanishes as time n progresses, the statistics of two successive samples can be viewed very close, i.e., $\sigma_e^2(n) = \sigma_e^2(n+1) = \sigma_e^2$, when the algorithm runs under convergence. Based on the above statement and

16

some mathematical manipulation, we have

$$L(n+1) - L(n) = -\frac{1}{2\tau_1} \ln \frac{\mu(n+1)\left(1 - \mu(n)\sigma_{x'}^2\right)}{\mu(n)\left(1 - \mu(n+1)\sigma_{x'}^2\right)}, \qquad (3.30)$$

and

$$R(n+1) - R(n) = -\frac{1}{2\tau_2} \ln \frac{\mu(n+1)\left(1 - \mu(n)\sigma_{x'}^2\right)}{\mu(n)\left(1 - \mu(n+1)\sigma_{x'}^2\right)}. \qquad (3.31)$$

Substituting (3.27) into (3.30) and (3.31), we obtain the recursive form for $L(n+1)$ and $R(n+1)$ as follows:

$$L(n+1) = L(n) - \frac{1}{2\tau_1} \ln \frac{(L(n-1) + R(n-1))\Phi(n-1) + \sigma_{x'}^2}{(L(n) + R(n))\Phi(n) + \sigma_{x'}^2}, \qquad (3.32)$$

$$R(n+1) = R(n) - \frac{1}{2\tau_2} \ln \frac{(L(n-1) + R(n-1))\Phi(n-1) + \sigma_{x'}^2}{(L(n) + R(n))\Phi(n) + \sigma_{x'}^2}. \qquad (3.33)$$

In practical use, the tap length is actually an integer number. Hence, we also need to round down $L(n+1)$ and $R(n+1)$ obtained from (3.32) and (3.33) to the nearest integers as the resultant.

The next question is whether the proposed recursion (3.32) and (3.33) can converge. Return to (3.13), it is known that for the two parameters $L(n+1)$, $R(n+1)$ and $\mu(n+1)$, the MSD is a convex function of them and the recursions will find minimum MSD if we can prove that $\frac{\partial \Lambda^2(n+1)}{\partial \mu^2(n+1)} > 0$, $\frac{\partial \Lambda^2(n+1)}{\partial L^2(n+1)} > 0$ and $\frac{\partial \Lambda^2(n+1)}{\partial R^2(n+1)} > 0$. Taking the second-order derivative of (3.13)

with respect to $\mu(n+1)$, $L(n+1)$ and $R(n+1)$, respectively, we have

$$\frac{\partial \Lambda^2(n+1)}{\partial \mu^2(n+1)} = 2\sigma_{x'}^2 (L(n+1) + R(n+1))\sigma_e^2(n) + 4\sigma_{x'}^4 (\Lambda(n) - \Gamma(n)), \quad (3.34)$$

$$\frac{\partial \Lambda^2(n+1)}{\partial L^2(n+1)} = 8\tau_1^2 \mu(n+1)\sigma_{x'}^2 (1 - \mu(n+1)\sigma_{x'}^2) \frac{\sigma_{r_w}^2 \left(-e^{-2L(n+1)\tau_1}\right)}{1 - e^{2\tau_1}}, \quad (3.35)$$

and

$$\frac{\partial \Lambda^2(n+1)}{\partial R^2(n+1)} = 8\tau_2^2 \mu(n+1)\sigma_{x'}^2 (1 - \mu(n+1)\sigma_{x'}^2) \frac{\sigma_{r_w}^2 e^{-2R(n+1)\tau_2}}{1 - e^{-2\tau_2}}. \quad (3.36)$$

In (3.34), $\Lambda(n) - \Gamma(n) \geq 0$ based on (3.29) and in (3.35) and (3.36), $1 - \mu(n+1) > 0$ in general situations. Therefore, the results of (3.34), (3.34) and (3.35) are all positive and then, we have shown that the MSD is a convex function of $L(n+1)$, $R(n+1)$ and $\mu(n+1)$, and consequently, the new variable tap length and step size FxLMS algorithm can converge to the minimum MSD.

Chapter 4   Practice Methods and On-line Secondary Path Systems

4.1   Proposed Algorithm with Online Secondary Path Estimation

In the previous section, the discussion is under the condition of $\widehat{S}(z) = S(z)$. However in practice, $\widehat{S}(z)$ is different from $S(z)$. In recent research the deviation of $\widehat{S}(z)$ from $S(z)$ can be reduced with online secondary estimation. Zhang's method [13] has better performance in online secondary estimation structure, which is considered for the application of the proposed algorithm.

The block diagram of the Zhang's method is depicted in Fig.4.1. The coefficients of $W(z)$ is updated by $e'(n)$, which differs from the traditional FxLMS and is expressed in the following:

$$e'(n) = d(n) - y(n) + u(n) - \hat{u}(n) + v(n), \tag{4.1}$$

where $u(n) = \varepsilon(n) * s(n)$, $\hat{u}(n) = \varepsilon(n) * \hat{s}(n)$. In order to investigate how the auxiliary noise $\varepsilon(n)$ affects the proposed algorithm on the online sec-

ondary path estimation FxLMS system, we set the background noise $v(n)$ to zero. The auxiliary noise $\varepsilon(n)$ is generated by white noise generator, which is used for $\widehat{S}(z)$ convergence. Using the same method to obtain (3.9), we have

$$
\begin{aligned}
e'(n) &= -\mathbf{x}'^T_K(n)\mathbf{g}_K(n) - \varepsilon(n) * (\mathbf{\hat{s}}(n) - \mathbf{s}(n)) \\
&= -\mathbf{x}'^T_K(n)\mathbf{g}_K(n) - (\hat{u}(n) - u(n)) \\
&= -\mathbf{x}'^T_K(n)\mathbf{g}_K(n) - \xi(n).
\end{aligned} \tag{4.2}
$$

The residual error $\xi(n)$ is obtained by the convolution output of the auxiliary noise $\varepsilon(n)$ and the deviation of $\widehat{S}(z)$ which equals $\hat{u}(n) - u(n)$. Then, in addition to σ_v^2 in (3.17), (3.23), (3.24), (3.25) and (3.26), σ_ξ^2 is added. Existing the deviation of $\widehat{S}(z)$ can make the convergence rate of $W(z)$ slower. When $\widehat{S}(z)$ converges to $S(z)$, the convergence of $W(z)$ will be not influenced.

In practice, $\widehat{S}(z)$ needs a initial value to speed up the convergence rate and reduces the influence for the convergence of $W(z)$. When the system structure and components, such as DAC, ADC, microphone, loudspeaker, etc., are fixed, an impulse signal into the DAC can be used to measure the impulse response of $S(z)$ as the output is received behind the ADC. In practical situation, the initial value of $\widehat{S}(z)$ can be obtained by some
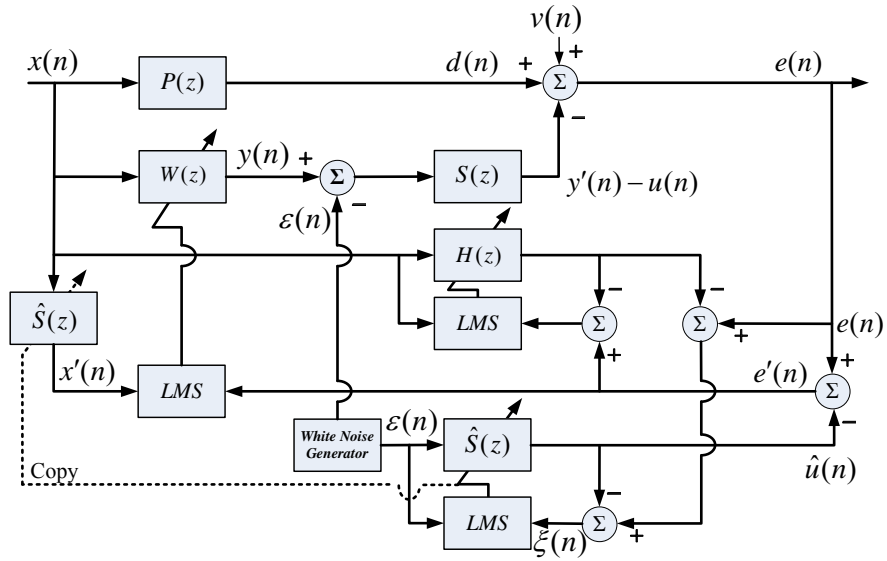
Figure 4.1: ANC system with online secondary-path estimation (Zhang's method).

methods.

However, when the location of the maximum impulse response output of $\widehat{S}(z)$ has the offset from that of $S(z)$, the convergence performance is seriously affected. We can evaluate the performance of Λ to correct the maximum output location of $\widehat{S}(z)$. The related results will be shown in the next section.

4.2 Proposed Algorithm Practice in Real System

In practice, the optimal coefficients $\mathbf{w}_K^o$ is unknown. And its the two hand side tap length M, N and the decaying factor τ_1, τ_2 are unknown as well, which directly affect the calculations of the tap length and the step

size in proposed algorithm. Next, we will introduce a method to get those parameters.

First, use the fixed tap length with large step size LMS algorithm, whose tap length is large enough to cover to the maximum power of impulse response of the unknown plant. After hundreds of times iteration, generally optimal coefficients of the $W(z)$ can be obtained. We express the generally optimal coefficients for $W(z)$ as follows:

$$\mathbf{w'}^{o}_{K'} = [w'^{o}_{-M'} \cdots \quad w'^{o}_{-1} \quad w'^{o}_{0} \quad w'^{o}_{1} \cdots w'^{o}_{N'-1}]^{T} \tag{4.3}$$

The K' is total tap length of the generally optimal coefficients $\mathbf{w'}^{o}_{K'}$, and the M' is left side tap length, and N' is right side tap length with maximum output of generally optimal coefficients.

Second, we inverse all of the $\mathbf{w'}^{o}_{K'}$ to positive. Then compare the two hand side adjacent coefficients in order to get the each peak value like $w'^{o}_{n-1} < w'^{o}_{n} > w'^{o}_{n+1}$, and others are set to zero. The peak coefficients can be express as follows :

$$\mathbf{p}^{o}_{K'} = [p^{o}_{-M'} \cdots \quad p^{o}_{-1} \quad p^{o}_{0} \quad p^{o}_{1} \cdots p^{o}_{N'-1}]^{T} \tag{4.4}$$

Then according to the 3.4, ignore the Gaussian random sequence and re-

verse the equation. We can rewrite the generally decaying factor

$$if p_i^o > 0, \tau_i' = \begin{cases} \frac{1}{i} \ln p_i^o, & i = -M, \cdots, -1 \\ \\ \frac{1}{-i} \ln p_{-i}^o, & i = 0, 1, \cdots, N-1. \end{cases} \quad (4.5)$$

Then take the average of τ_i' with two hand side in order to obtain the generally decaying factor τ_1' and τ_2'. Substitute τ_1', τ_2', M' and N' into 3.20, 3.21, 3.22, 3.23 and 3.24.

Third, we can use the the two hand side ℓ_2 norm of the last 10 grown taps are less than threshold L' and R' for the two hand side to terminate the growth of the tap length.

Next, a real system simulation will be shown in the next section.

23
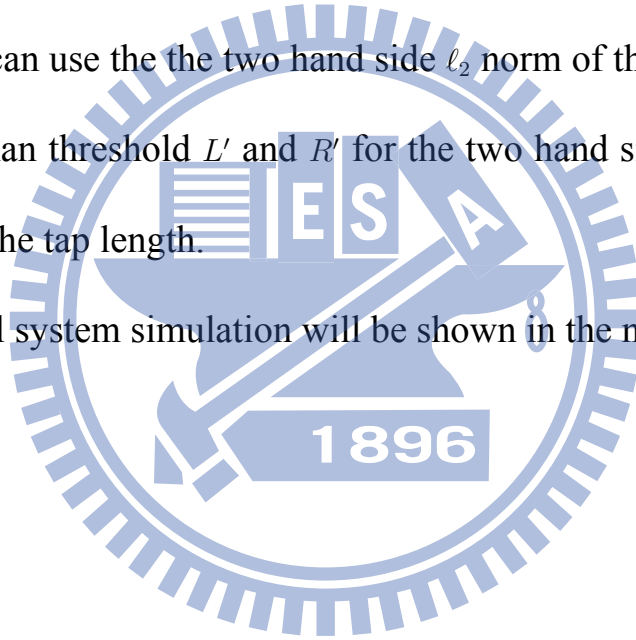
Chapter 5   Simulation Results

5.1   Proposed Algorithm on FxLMS

In this section, some computer simulations are employed to compare ANC performance of the proposed algorithm with different FxLMS algorithms. The secondary path model $S(z)$ includes the loudspeaker and microphone system, and according to [8], a filter is used to model the secondary path model $S(z)$ and the frequency response is shown in Fig.5.1. We set the impulse response length of plant $P(z)$ as 1088 and the length of the loudspeaker model $S(z)$ as $L = 65$. Hence, a proper length for the optimal impulse response $W^o(z)$ of $W(z)$ is $K = 1024$. For simplicity, we let $\widehat{S}(z)$ equal $S(z)$ and generate $P(z)$ from $P(z) = W^o(z)S(z)$ and the impulse response is shown in Fig.5.2. Once the estimate $\widehat{W}(z)$ of $W(z)$ is obtained, the MSD can be easily evaluated through 100 Monte Carlo simulations by calculating $\|\hat{\mathbf{w}}(n) - \mathbf{w}_K^o(n)\|_2^2$ for each iteration. Other simulation setups include that $r_w(i)$ was generated by a zero-mean white Gaussian random process with variance $\sigma_{r_w}^2 = 0.01$; the exponential decaying factor τ_1 and τ_2 were 0.01 and 0.005; and the reference noise and the background noise were zero-mean i.i.d. and uncorrelated Gaussian processes with variances $\sigma_x^2 = 1$ and $\sigma_v^2 = 0.01$, respectively.
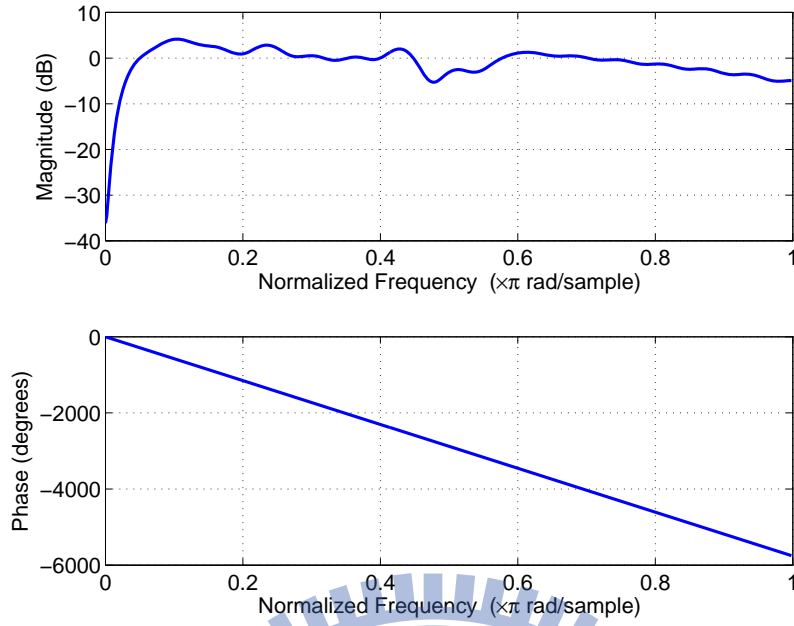
Figure 5.1: Frequency response of S(z).

In Fig. 5.3, the comparison of the MSD performance in decibel (dB) is shown for 50000 iterations. Since the tap length of $W^o(z)$ is 1024, we choose the same tap length for the typical FxLMS algorithm with large and small step sizes, where the large step size, according to (2.7), is set as $\mu_{\max} = \frac{1}{(1024+2) \times \sigma_{x'}^2}$ and the small step size $\mu_{\min} = 0.2\mu_{\max}$ because $\mu_{\min}$ provides the 1024-tap FxLMS algorithm a steady-state performance close to the proposed algorithm in 50000 iterations. A 1024-tap FxLMS algorithm with variable step size which is similar to [8] is also compared by using

$$\mu(n) = \rho(n)\mu_{\max} + (1 - \rho(n))\mu_{\min} \tag{5.1}$$

where $\rho(n)$ is a weighting factor, $0 \le \rho(n) \le 1$, and is calculated by $\rho(n) =$

25
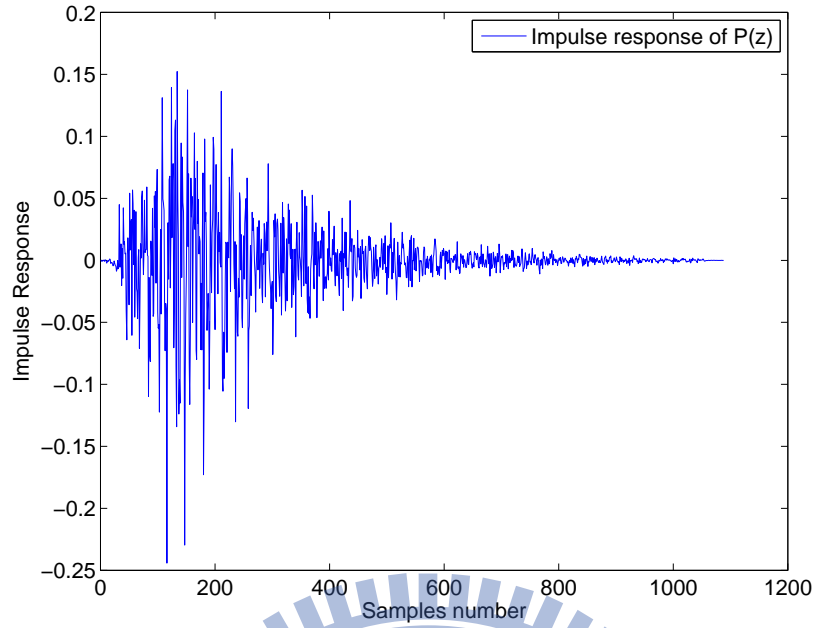
Figure 5.2: Impulse response of P(z).

$\frac{P_e(n)-P_{e,\min}}{P_{e,\max}-P_{e,\min}}$ with $P_{e,\max}$ and $P_{e,\min}$ representing the maximum and minimum average powers of $e(n)$, respectively and $P_e(n) = \frac{1}{T}\sum_{i=n-T+1}^{n} e^2(n)$ where T is an averaging constant with $T = 200$ herein. The maximum average power $P_{e,\max}$ uses the average of the first 100 iterations of $P_e(n)$ multiplied by 1.3 and minimum average power $P_{e,\min}$ uses the average of the last 100 iterations of $P_e(n)$ multiplied by 0.7. From Fig. 5.3, we can find that the proposed algorithm has a much faster convergence rate than other algorithms. However, if we set a fixed step size $\mu_{\max}$ for the proposed algorithm, the converged MSD performance becomes worse in spite of the same convergence rate. Although the variable step size FxLMS has a better convergence rate than the large step size FxLMS and a better converged performance than the small step size FxLMS, its step size is
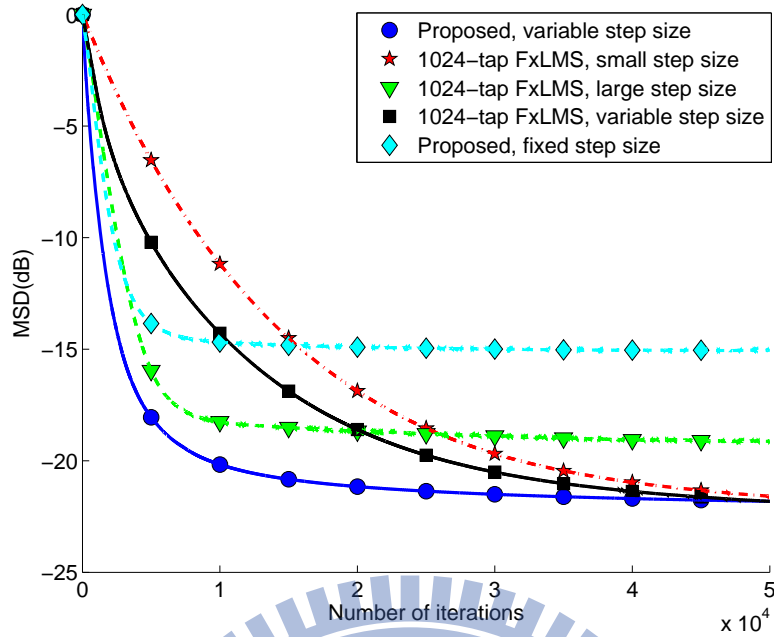
26

Figure 5.3: Comparison of the MSD convergence performance for different algorithms.

somewhat heuristic such that the overall performance is worse than the proposed algorithm. By terminating the growth of the left tap length when the ℓ_2 norm of the last 10 grown taps is less than 10^{-2} and 10^{-5} for the right-side, the total tap length approaches the number about 1104 as shown in Fig. 5.4(a), however, the MSD performance almost saturates as the variable step size can still decrease slowly as shown in Fig. 5.4(b).

An experiment to see the transient effect of noise reduction using the proposed algorithm is shown in Fig. 5.5. Suppose the input noise $x(n)$ is exacerbated with variance $\sigma_x^2 = 16$ from the $25000th$ to the $40000th$ iteration as shown in Fig. 5.5(a). From Fig. 5.5(b), the ANC output remains its residual error approaching the background noise level. To
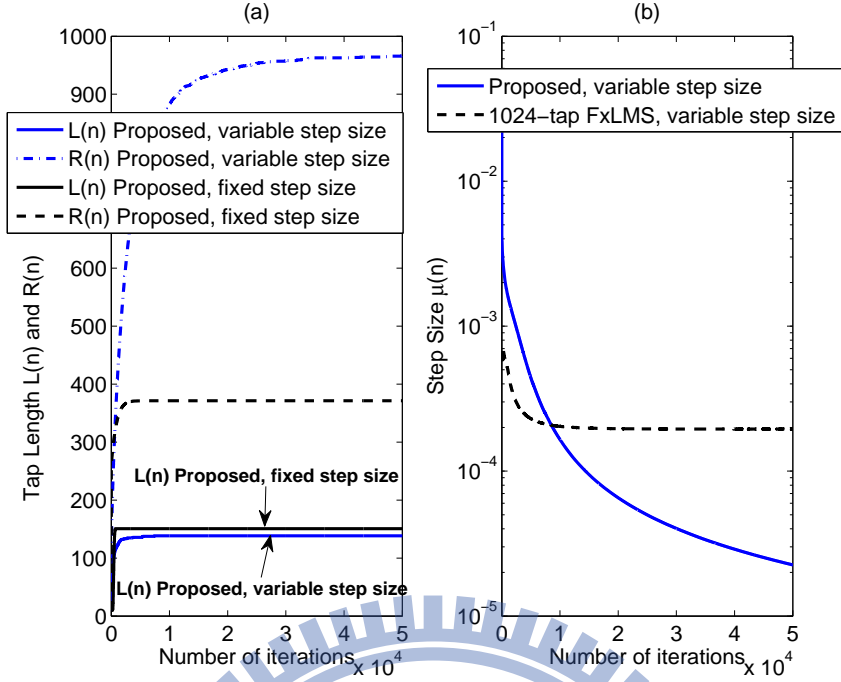
27

Figure 5.4: Convergence comparison of tap-length and step size for proposed algorithm and other FxLMS algorithms: (a) Tap length $M(n)$; (b) Step size $\mu(n)$.

evaluate the noise reduction performance for ANC, we define an index, noise reduction ratio NRR (dB), which is given by

$$\text{NRR(dB)} = 10\log\left(\frac{E[d^2(n)]}{E[e^2(n)]}\right), \qquad (5.2)$$

where $E[\cdot]$ can be evaluated by ensemble average for simplicity. By NRR (dB), Fig. 5.6 plots the comparison of the proposed algorithm with other algorithms. In addition to a better MSD performance, the proposed algorithm has the superior NRR (dB) performance for the ANC application because of its fast convergence property.
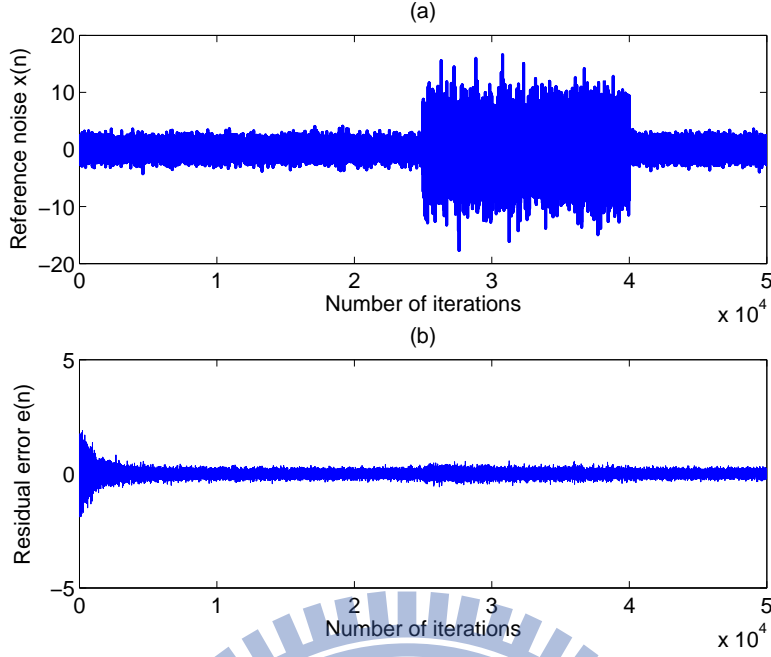
Figure 5.5: The transient effect of noise reduction: (a) Input reference noise $x(n)$; (b) Residual error $e(n)$.

5.2 Proposed Algorithm on Online Secondary Path Modeling FxLMS

We have two simulations about effect of $\widehat{S}(z)$. The online secondary path modeling is based on Zhang's method like Fig.4.1. The auxiliary noise $\varepsilon(n)$ was zero-mean i.i.d. and uncorrelated Gaussian processes with variances $\sigma_\xi^2 = 1$. The initial value of $\widehat{S}(z)$ uses the $\mathbf{s}(n)$ with weighted standard deviation $(0.5*s(n))^2)$ of Gaussian random noise. The step size of $\widehat{S}(z)$ was set to $\mu_s = \frac{0.045}{(65+2)\sigma_v^2}$, and the step size $H(z)$ was set to $\mu_h = \frac{0.01}{(1024+2)\sigma_x^2}$, and the other parameters were the same previous simulation.

In the first simulation, we compare with two initial values of $\widehat{S}(z)$, one
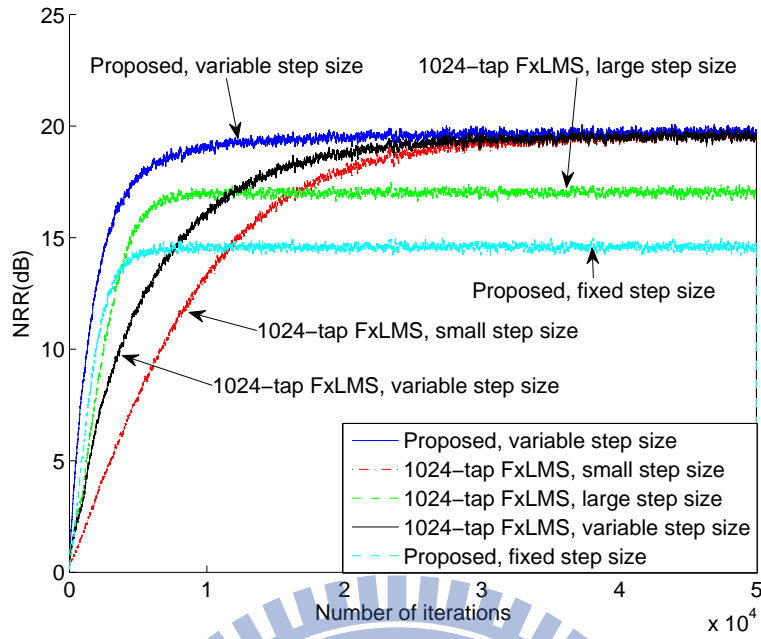
Figure 5.6: Comparison of NRR (dB) performance for different ANC algorithms.

is $s(n)$, and the other one is $s(n)$ with weighted random noise. As Fig.5.7, the variance of auxiliary noise σ_ξ^2 affects the step size(3.26) during the convergence. Although the $\widehat{S}(z)$ is almost the same as the $S(z)$ at about 10000 iterations. That effect causes slightly different convergence speed, which make the MSD have a little offset at the end of simulation.

In the second simulation, we shift the maximum power center of initial value of $\widehat{S}(z)$ with one tap on two-hand sides,each for five times. As Fig.5.8, no matter which side the maximum power center is shifted to or no matter how many taps, Λ and MSD are very poor. However, when the maximum power center is aligned, the Λ and MSD are the best.

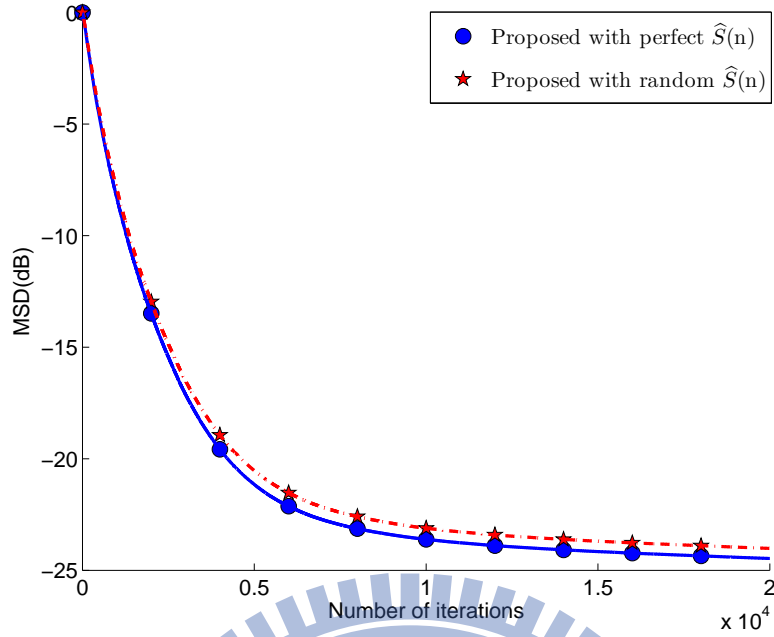To setup an appropriate variance of auxiliary noise, we run two sim-

Figure 5.7: The MSD of proposed algorithm with online secondary path modeling.

ulations: one is to change different variances of background noise on the traditional FxLMS, and the other one is to change different variances of auxiliary noise on the Zhang's method of online secondary path modeling FxLMS. In the first one, the variance of background noise σ_v^2 takes ten numbers that make the SNR($10log(\frac{\sigma_d^2}{\sigma_v^2})$) from 40dB to 2dB. Then we compare the steady-state MSD of proposed algorithm in Fig.5.9. In the second, the variance of auxiliary noise σ_ε^2 takes eleven numbers that make the SNR($10log(\frac{\sigma_d^2}{\sigma_\varepsilon^2})$) from 10dB to -10dB. Then we compare the steady-state MSD of proposed algorithm on online secondary path modeling FxLMS in Fig.5.10.

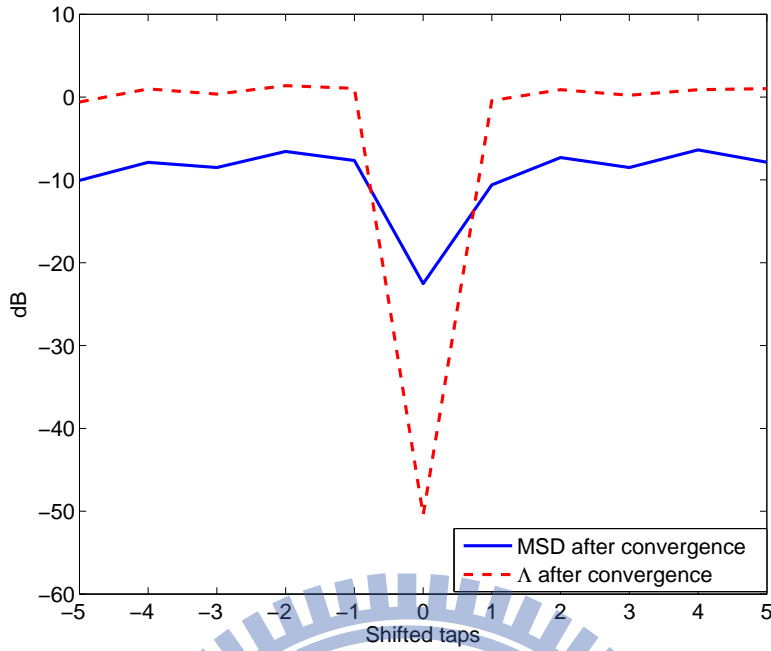The $v(n)$ and the $\varepsilon(n)$ respectively in the traditional FxLMS and the on-

Figure 5.8: The average of MSD and Λ of $W(z)$ with different shifted maximum power center.

line secondary path modeling FxLMS affect the covergence. In Fig.5.9, when the SNR is smaller than 25dB, the steady-state MSD of proposed algorithm is better than the others. According the Fig.5.7 and Fig.5.10, the smaller auxiliary noise makes the convergence of $\widehat{S}(z)$ slower and indirectly makes the convergence of $W(z)$ slower. However, in the Fig.4.1, because the residual error $e(n)$ includes the $\varepsilon(n) * s(n)$, the larger auxiliary noise makes the residual error $e(n)$ larger, too. Therefore, the variance of auxiliary noise σ_ε^2 can not be set too large within the acceptable convergence speed, so selecting SNR between 0dB to -6dB is the better choice in this case.
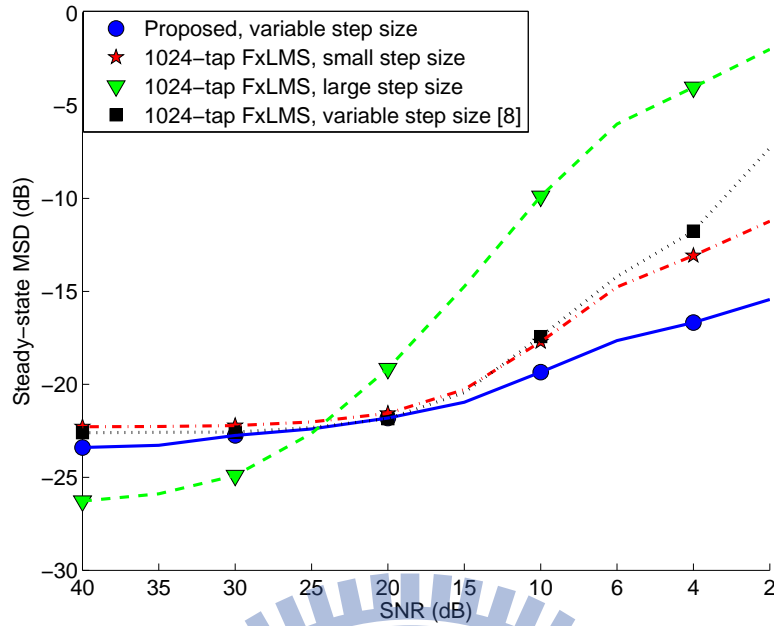
Figure 5.9: The steady-state MSD of different variances of background noise v(n).

5.3 Proposed Algorithm Practice in Real System on Online Secondary Path Modeling FxLMS

In accordance with the method described in the previous section, we use a real system of $P(z)$ and $S(z)$ to verify the proposed algorithm. The impulse response and frequency response of $P(z)$ are shown as Fig.5.11 and Fig.5.12:

And the impulse response of $S(z)$ is shown as Fig.5.13. The impulse response sample length of $P(z)$ and $S(z)$ are 145 and 51 taps. Based on these, the optimal coefficients of $W(z)$ is 95 taps.
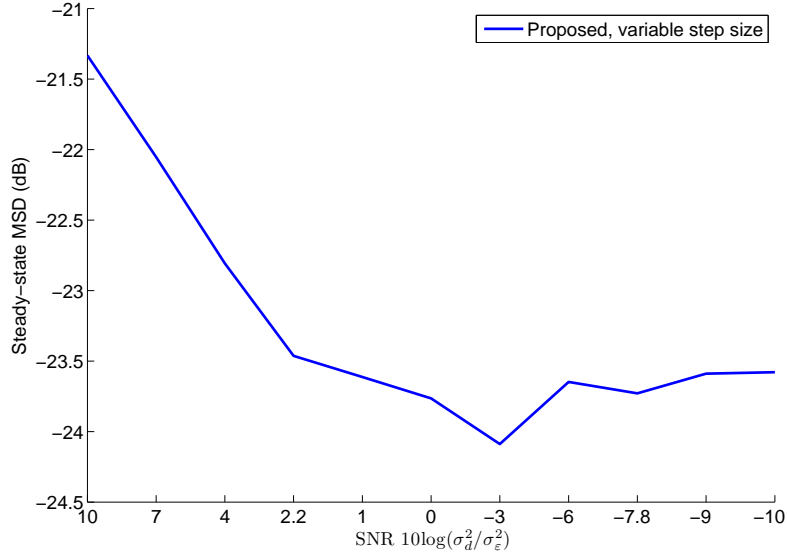
Figure 5.10: The steady-state MSD of different variances of auxiliary noises $\varepsilon(n)$.

The simulation is to compare noise reduction ratio NRR (dB) of proposed algorithm with different on online secondary path modeling FxLMS algorithms shown in Fig.5.14, Fig.5.15 and Fig.5.16. The NRR definition of the on online secondary path modeling FxLMS is different from traditional FxLMS, which is given by

$$\text{NRR(dB)} = 10\log\left(\frac{E[d^2(n)]}{E[e'^2(n)]}\right). \tag{5.3}$$

About the proposed algorithm setting, the generality optimal coefficients parameters M' and N' are set to 64 and 316, the τ'_1 and τ'_2 are set to 0.0925 and 0.0626. The terminating threshold L' and R' are set to 10^{-1} and 5×10^{-4}. About the normalized LMS(NLMS) algorithm [2] setting, the smoothing
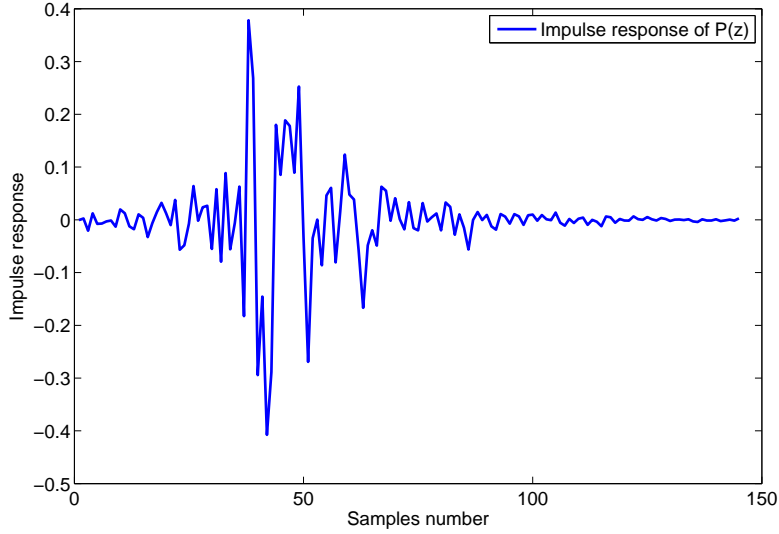
Figure 5.11: The impulse response of real P(z).

parameter is set to 0.99, the normalized step size α is set 0.4 and the tap length L is set to 95. We use two 95-taps FxLMS algorithms one with a large step size and the other with the small step size, where the large step size is set as $\mu_{\max} = \frac{1.2}{(95+2) \times \sigma_{x'}^2}$ and the small step size $\mu_{\min} = \frac{0.4}{(95+2) \times \sigma_{x'}^2}$. A 95-taps FxLMS with variable step size is similar to [8], whose the parameters $\rho, P_e, P_{e,\min}$ and $P_{e,\max}$ are the same as the previous traditional FxLMS simulation, and the maximum and minimum step sizes are between the other two 95-taps FxLMS with large and small step size.

In Fig.5.14, we adjust the final performance of proposed algorithm, NLMS [2], variable step size [8] and 95-taps FxLMS with small step size are close, and then compare the convergence speeds. The step size of the 95-taps FxLMS with large step size is adjusted so that its convergence speed is as close to proposed algorithm as possible, and then compare the
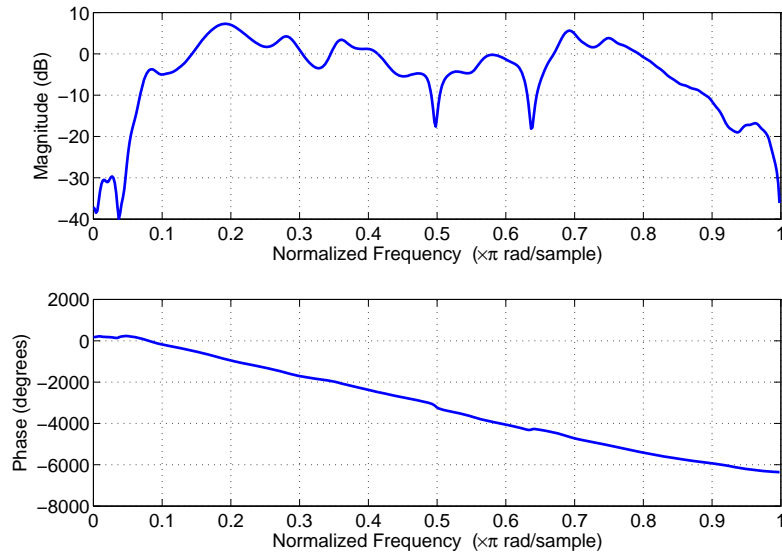
35

Figure 5.12: The frequency response of real P(z).

final performance.

In Fig.5.15, the convergence speed of proposed algorithm is better than the NLMS [2], variable step size [8] and 95-taps FxLMS with small step size. The final performance of proposed algorithm is better than the 95-taps FxLMS with large step size.

In Fig.5.16(a), the tap length of proposed algorithm is terminated at 92 taps, which is close the tap length of optimal coefficients 95 taps. Shown in Fig.5.16(b), the step size of proposed algorithm gradually decreases slower than the others.
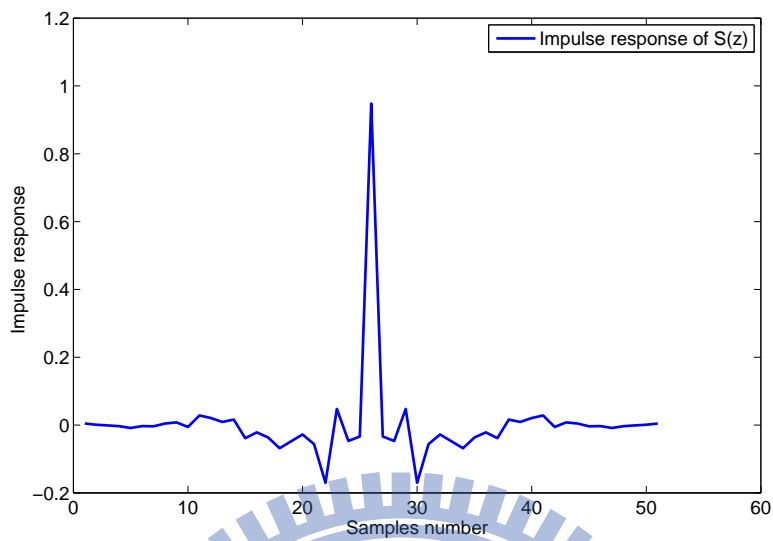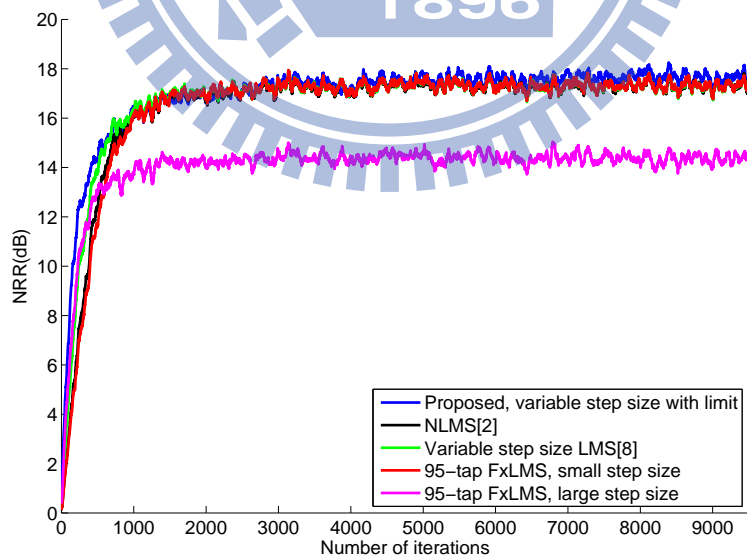
Figure 5.13: The impulse response of real S(z).

Figure 5.14: Comparison of NRR (dB) performance for different online secondary path modeling FxLMS algorithm.
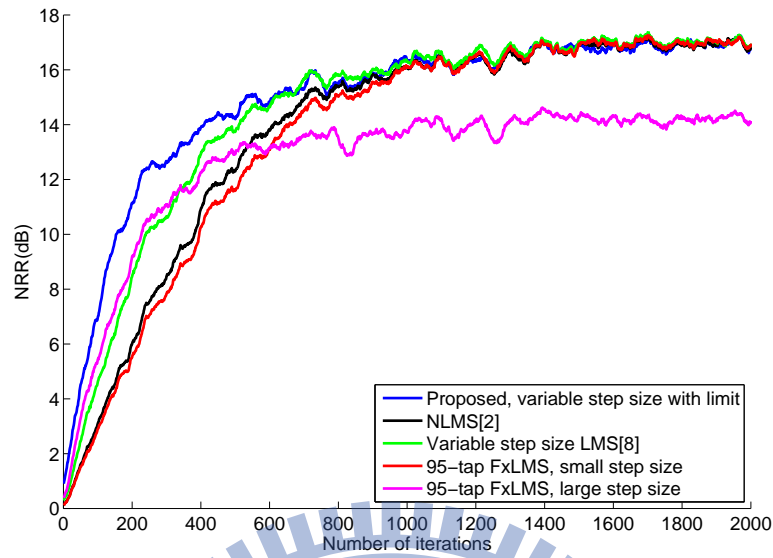
Figure 5.15: The result of the comparison of NRR (dB) performance for different online secondary path modeling FxLMS algorithm before 2000 iterations.
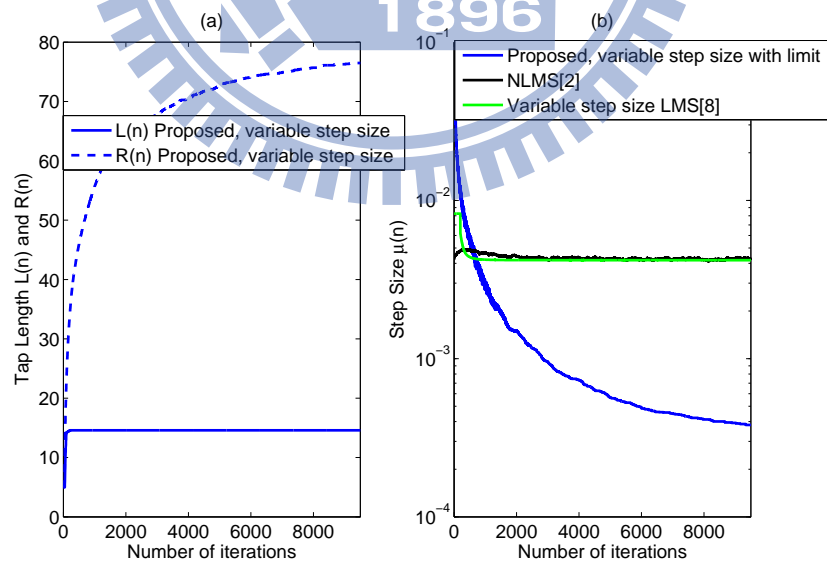

Figure 5.16: Convergence comparison of tap-length and step size for proposed algorithm and other online secondary path modeling FxLMS algorithms: (a) Tap length $M(n)$; (b) Step size $\mu(n)$.

38

Chapter 6   Conclusion

We propose a new ANC system using a variable tap length and step size FxLMS algorithm where a simple recursive form is obtained as well to estimate the tap length. Here, the new FxLMS algorithm is developed based on the assumption that the impulse response of the control filter in the ANC secondary path has an unsymmetric and exponential decaying enve- lope in order to deal with the lowpass filter in the loudspeaker system. The proposed FxLMS algorithm has a much faster convergence rate than the conventional and variable step size FxLMS algorithms without intensively computational cost of implementing complicated DFT or subband filters.
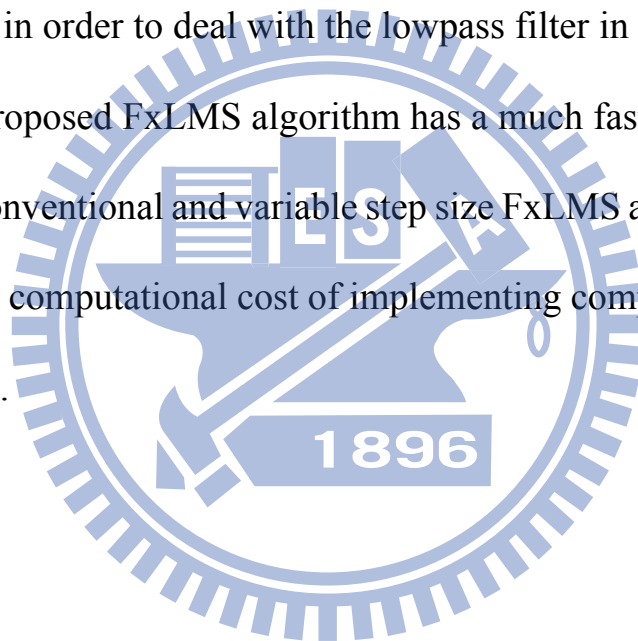
References

[1] S. J. Elliott and P. A. Nelson, "Active noise control,"*IEEE Signal Processing Magazine*, vol. 10, no. 4, pp. 12 –35, Oct. 1993.

[2] S. M. Kuo and D. R. Morgan, *Active Noise Control Systems - Algorithms and DSP Implementations*.   New York: Wiley, 1996.

[3] D. R. Morgan, "An analysis of multiple correlation cancellation loops with a filter in the auxiliary path,"*IEEE Trans. Acoust., Speech, Signal Process.*, vol. ASSP-28, no. 4, pp. 454 –467, Aug. 1980.

[4] S. M. Kuo and J. Luan, "Cross-coupled filtered-x LMS algorithm and lattice structure for active noise control systems,"in *IEEE International Symposium on Circuits and Systems (ISCAS '93)*, May. 1993, pp. 459 –462.

[5] S. J. Park, J. H. Yun, Y. C. Park, and D. H. Youn, "A delayless subband active noise control system for wideband noise control,"*IEEE Trans. Speech Audio Process.*, vol. 9, no. 8, pp. 892 –897, Nov. 2001.

[6] M. Wu, X. Qiu, and G. Chen, "An overlap-save frequency-domain implementation of the delayless subband ANC algorithm,"*IEEE Trans. Audio, Speech, Language Process.*, vol. 9, pp. 1706 –1710, Nov. 2008.

[7] G. Long, F. Ling, and J. G. Proakis, "Corrections to 'The LMS algorithm with delayed coefficient adaption',"*IEEE Trans. Signal Process.*, vol. 40, no. 1, pp. 230 –232, Jan. 1992.

[8] M. T. Akhtar, M. Abe, and M. Kawamata, "A new variable step size LMS algorithm-based method for improved online secondary path modeling in active noise control systems,"*IEEE Trans. Speech Audio Process.*, vol. 14, no. 2, pp. 720 –726, Mar. 2006.

[9] Y. Gu, K. Tang, H. Cui, and W. Du, "Convergence analysis of a deficient-length LMS filter and optimal-length sequence to model exponential decay impulse response,"*IEEE Signal Process. Letters*, vol. 10, pp. 4 –7, Jan. 2003.

[10] Y. Zhang, J. A. Chambers, S. Sanei, P. Kendrick, and T. J. Cox, "A new variable tap-length LMS algorithm to model an exponential decay impulse response,"*IEEE Signal Process. Letters*, vol. 14, no. 4, pp. 263 –266, April 2007.

[11] K. Shi, X. Ma, and G. T. Zhou, "A variable step size and variable tap length LMS algorithm for impulse responses with exponential power profile,"in *Proc. ICASSP*, April 2009, pp. 3105 –3108.

[12] M. Zhang, H. Lan, and W. Ser, "On comparison of online secondary path modeling methods with auxiliary noise,"*IEEE Trans. Speech Audio Process.*, vol. 13, no. 4, pp. 618 –628, July 2005.

[13] M. Zhang, H. Lan, and W. Ser, "Cross-updated active noise control system with on-line secondary path modeling,"*IEEE Trans. Speech Audio Process.*, vol. 9, no. 5, pp. 598 –602, July 2001.

Vita

Fei-Tao Chu was born in Taiwan R.O.C., in 1978. He received the B.S. degree in Computer Science and Information Engineering from Chung Hua University.

From June 2000 to January 2012, serving in AVID Electronics Corp, ELAN Microelectronics Corp. and WYS SoC Corp., he was engaged in the researches of the audio signal processing.

In 2013, he got the M.S. degree in the Institute of Communications Engineering in National Chiao Tung University, Hsin-Chu, Taiwan. His research interests include active noise cancellation and adaptive filtering.